

Precise determination of the zero-gravity surface figure of a mirror without gravity-sag modeling

Eric E. Bloemhof,* Jonathan C. Lam, V. Alfonso Feria, and Zensheu Chang
Jet Propulsion Laboratory, California Institute of Technology, Pasadena, California 91109, USA

*Corresponding author: eric.e.bloemhof@jpl.nasa.gov

Received 29 June 2007; accepted 10 August 2007;
posted 29 August 2007 (Doc. ID 84671); published 25 October 2007

The zero-gravity surface figure of optics used in spaceborne astronomical instruments must be known to high accuracy, but earthbound metrology is typically corrupted by gravity sag. Generally, inference of the zero-gravity surface figure from a measurement made under normal gravity requires finite-element analysis (FEA), and for accurate results the mount forces must be well characterized. We describe how to infer the zero-gravity surface figure very precisely using the alternative classical technique of averaging pairs of measurements made with the direction of gravity reversed. We show that mount forces as well as gravity must be reversed between the two measurements and discuss how the St. Venant principle determines when a reversed mount force may be considered to be applied at the same place in the two orientations. Our approach requires no finite-element modeling and no detailed knowledge of mount forces other than the fact that they reverse and are applied at the same point in each orientation. If mount schemes are suitably chosen, zero-gravity optical surfaces may be inferred much more simply and more accurately than with FEA. © 2007 Optical Society of America

OCIS codes: 000.2780, 120.6650, 220.4840.

1. Introduction: Optics for Spaceborne Observatories

The Space Interferometry Mission (SIM) PlanetQuest under development at the Jet Propulsion Laboratory (JPL) will provide unprecedented astrometry that in turn will reap unprecedented scientific dividends in numerous areas of astronomy, from setting fundamental size scales of the universe to studying extrasolar planets [1]. The technological demands of operating an optical interferometer in space are formidable ([2] and references therein). Front-end (collector) optics in each arm of the interferometer comprise an articulating flat siderostat, a three-element compressor, a flat fast-steering mirror that is conjugate to the pupil defined by the siderostat, and flat relay optics that route starlight to an interferometric beam combiner. The overall wavefront quality requirement is very challenging, ~ 37 nm rms over a rather large field of view, $1^\circ \times 0.1^\circ$. The compressor is therefore a three-mirror anastigmat [3], the only configuration with enough design degrees of freedom

to meet this wavefront budget. Maintaining high wavefront quality is most difficult on large, powered optics, and so interest naturally centers on fabrication and testing of the primary mirror, M1, the largest mirror in the compressor. The flight design for M1 is an off-axis paraboloid (OAP) fabricated from ultra-low-expansion (ULE) glass, with lightweighting pockets in the back of the mirror to save launch mass. The flight wavefront error budget allotment to M1 is an ~ 8 nm rms manufacturing error plus deformation due to mounting, as part of the allotment of wavefront error for the SIM collector assembly as a whole. This wavefront number refers to departures from nominal optical surface figure in zero gravity, after the SIM is launched. There are also requirements on the surface figure in normal gravity to assist in integration and test before launch, but the key testing challenge is inferring the zero-gravity figure of off-axis paraboloids and other powered optics from surface metrology performed on the ground, in normal gravity.

Flight versions of M1 will not be produced for several years, but two different test versions will have preceded it to provide experience with the thermo-

0003-6935/07/317670-09\$15.00/0
© 2007 Optical Society of America

opto-mechanical behavior of the glass and mount designs. The first of these is the “brassboard” M1, completed in 2005. The brassboard M1 was incorporated in the sophisticated TOM3 testbed [4] that emulated one arm of a SIM interferometer and studied its optical behavior with temperature variations. This brassboard M1 was a flightlike OAP. The second test version of M1 is the “prototype,” PT-M1, ~343 mm in diameter, completed in April 2007. For simplicity, PT-M1 has a simpler spherical figure, with a radius of curvature of ~2.2 m, though it has a flightlike surface quality spec of 6.3 nm rms ($\lambda/100$ rms) under zero-gravity conditions. It is also aggressively lightweighted in a flightlike way (Fig. 1), resulting in a weight of 3.875 kg and an areal density of 41.9 kg m⁻². In addition to basic acceptance testing of the bare mirror itself used to illustrate the concepts presented in this paper, PT-M1 is being tested in a flightlike mount consisting of three bipods bonded to the mirror hub. Its surface figure in that configura-

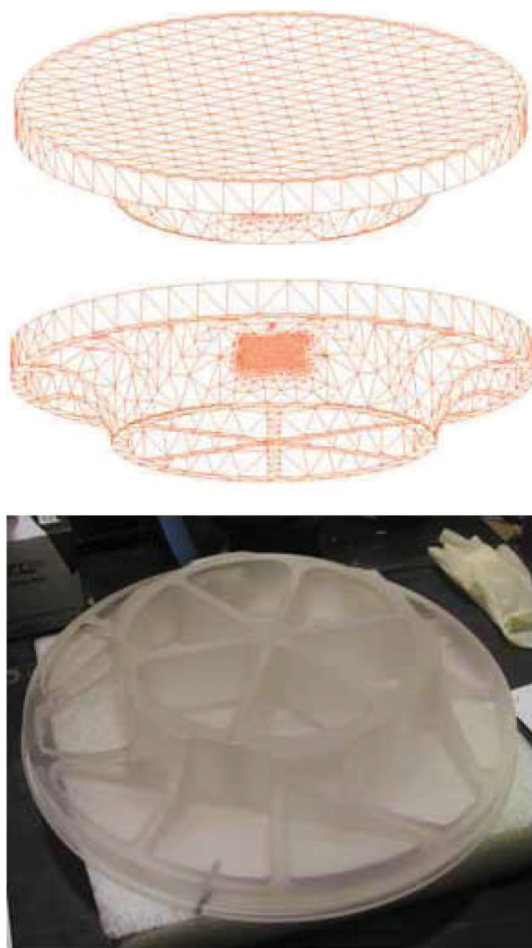


Fig. 1. (Color online) Views of front (top) and back (middle) of PT-M1, a prototype of the primary mirror for SIM's three-mirror compressor. The mirror is 343 mm in diameter and has a spherical surface with radius of curvature ~2.2 m. Nodes for FEA modeling are shown, and bonding pads for attaching hexapod mounts are visible. At the bottom is a photograph of the mirror during fabrication, showing details of backside lightweighting. [Photograph courtesy S. Spanjian and J. Daniel, Tinsley.]

tion will again be monitored by surface metrology with a commercial Fizeau interferometer for potential changes following temperature cycling and mechanical vibration testing.

2. Gravity Sag and Dimples in Ground-Based Tests

High-precision mirror surface measurements under normal gravity are very sensitive to details of the mount fixture. These issues are well illustrated by experience with the TOM3 brassboard M1 primary mirror. The flightlike mount consisted of an elaborate system of stiff hexapods and a soft offload ring, resulting in minimal mount stresses in the glass; so if the mirror had the correct zero-gravity figure it would have demonstrated that figure when installed in the flight mount, apart from a gravity-sag pattern of low spatial frequency. However, due to tight schedule constraints, it was decided to monitor surface quality during final polishing of the brassboard M1 by mounting the mirror on edge in a relatively crude mount consisting of two pegs making point contact under two edges of the lightweighting structure, with no gravity-reversal testing. Polishing in the flightlike mount was not possible, as that mount was not available. As a result, when later installed in the flightlike mount, the brassboard M1 exhibited a distinctive “print-through” error-map pattern featuring undesirable “dimples,” or localized surface defects (see Fig. 2), distributed with threefold symmetry and having amplitudes exceeding 100 nm [5]. (This pattern actually had little impact on the successful achievement of the critical milestones of the TOM3 testbed.) Though a two-point mount was used during fabrication, threefold symmetry presumably arose from the threefold symmetry of the brassboard M1's lightweighting design and of its flightlike mount. Overall surface error was 20 nm rms. A plausible explanation of the dimpling was developed: final polishing delivered a good parabolic surface in the presence of forces induced by the simple fabrication-cycle two-peg mount, and when these forces were removed in the flightlike mount, the glass surface relaxed into a shape suggesting the inverse pattern of stresses. The theoretical validation of this picture with finite-element analysis (FEA) is also shown in Fig. 2.

The dimpling experienced with the brassboard M1 was not a serious issue for the TOM3 testbed but would not be acceptable in the longer term for the flight M1 primary, with its zero-gravity surface spec of ~6.3 nm rms. It underscores the value of a simple and accurate way to extract the zero-gravity surface figure of an optic from tests made in normal gravity. FEA of the sort used to diagnose the dimples in the TOM3 brassboard M1 can certainly provide a way, in principle, to infer zero-gravity surfaces. However, experience shows FEA models may have errors of several tens of percent. Accurate results require accurate knowledge of mount forces, which can be difficult to ascertain. Peak deformations under gravity may be particularly substantial for aggressively lightweighted mirrors, in which case significant frac-

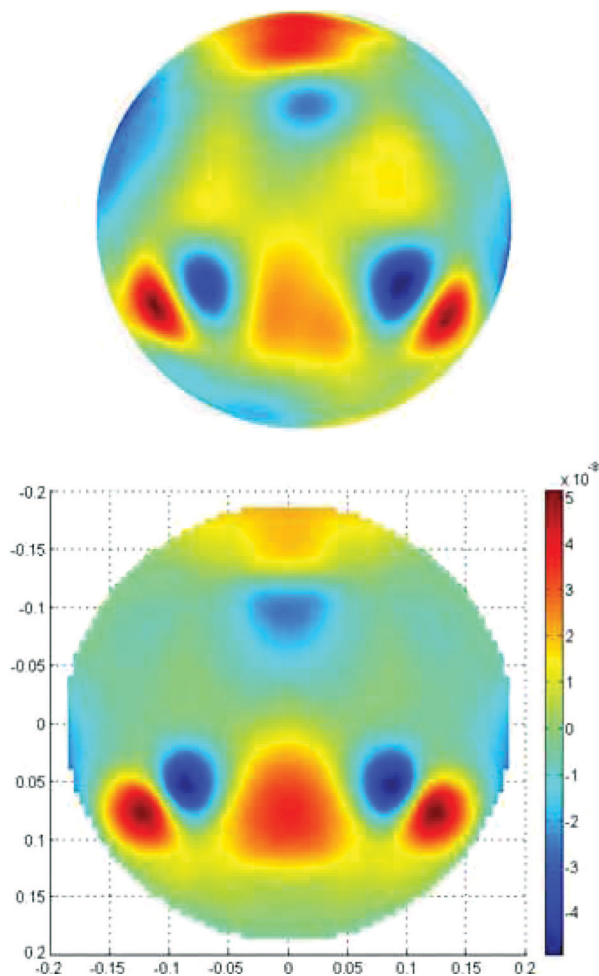


Fig. 2. (Color online) Mount-induced print-through (dimples) on the TOM3 brassboard model M1, as measured (top) and as simulated with a detailed FEA model (bottom). (From [5]; color-bar units in this and all later figures are meters.) The detailed origin of the dimples is discussed in the text, Section 2. The surface map here describes a normal-gravity on-edge configuration, and includes gravity sag in brassboard M1's flightlike mount in addition to the deformation caused by the fabrication mount. Surface errors on the measured map amount to 20 nm rms, with peaks exceeding 100 nm. The FEA model has 98,000 nodes and 49,000 elements and provides an excellent qualitative match but predicts a surface error of 14 nm rms. Since flight tolerance for this optic is ~ 6.3 nm rms, dimpling of this magnitude would not be permissible in the ultimate flight mirror.

tional FEA errors imposed on these large gravity sag distortions give large absolute errors.

As a starting point, and to lay out the principles of the problem, the methodology of FEA may be used to formulate a criterion that in principle allows the use of normal-gravity measurements to judge when the mirror will conform to a desired figure in zero gravity. A detailed FEA model of the mirror is required, with the desired zero-gravity surface figure specified, and also detailed modeling of how the mount interfaces with the mirror. The FEA simulation for this system in the mount and under the gravity orientation of the desired measurement configuration is then run to determine, for the desired zero-gravity surface, the

corresponding distorted, normal-gravity surface figure, which for the purposes of this discussion may be termed the "template." Then, to be sure the optic's zero-gravity surface figure lies within some given rms tolerance of the figure desired, the normal-gravity surface figure actually measured must lie within that same rms tolerance of the template. Put a different way, the error map for the measurement compared to the template, which is the normal-gravity surface obtained from the desired zero-gravity surface by FEA modeling of distortions due to gravity sag and mount forces, is the same error map describing the actual zero-gravity surface compared to the desired surface. This comparison procedure has to work at any gravity orientation. As mentioned, the main difficulty is getting detailed and accurate models of the mount forces, and so quantitative agreement with experiment is often only approximate. An alternative technique, based on symmetry under force reversal, is presented in Section 3.

3. Obtaining the Zero-Gravity Surface from Gravity-Reversed Measurement Pairs

A classic optical technique for extracting the zero-gravity surface figure averages two measurements made with the mirror turned in opposite orientations so that body forces due to gravity are reversed in the frame of the mirror. An example is shown in Fig. 3, with a very detailed FEA model representing the spherical PT-M1 in "face-up" and "face-down" orientations. This choice of mount configuration is simple but does not follow the principles to be laid out in Section 4 that guarantee that mount forces reverse to a high accuracy, along with gravity. Instead, mount forces in the two orientations are applied at the front and the back of the mirror rim and so reverse in direction but do not act at the same positions on the mirror. There is some cancellation of surface displacements in the two orientations, but it is by no means perfect. Surface deformations are 90 and 83 nm rms in the face-up and face-down orientations, respectively; residual errors in the average of the two are ~ 11.5 nm rms and manifest themselves as distinct dimpling near the periphery. This example clearly illustrates that reversing gravity is necessary but not sufficient for the gravity-reversal approach to work well. The spatial character of the errors suggests immediately that the problem is related to how the mirror is mounted in the two orientations. In Subsection 4.C and Section 5 we will propose alternative mounting schemes that address these problems and show that they result in much more accurate determinations of the zero-gravity surface figure.

4. Optimizing Zero-Gravity Measurements: Reversing Mount Forces

It is convenient to study theoretically the effects of gravity sag with the methods and notation of FEA. FEA will also be used to validate mounting schemes that may be expected to work well from first principles. Note, however, that the method for effectively

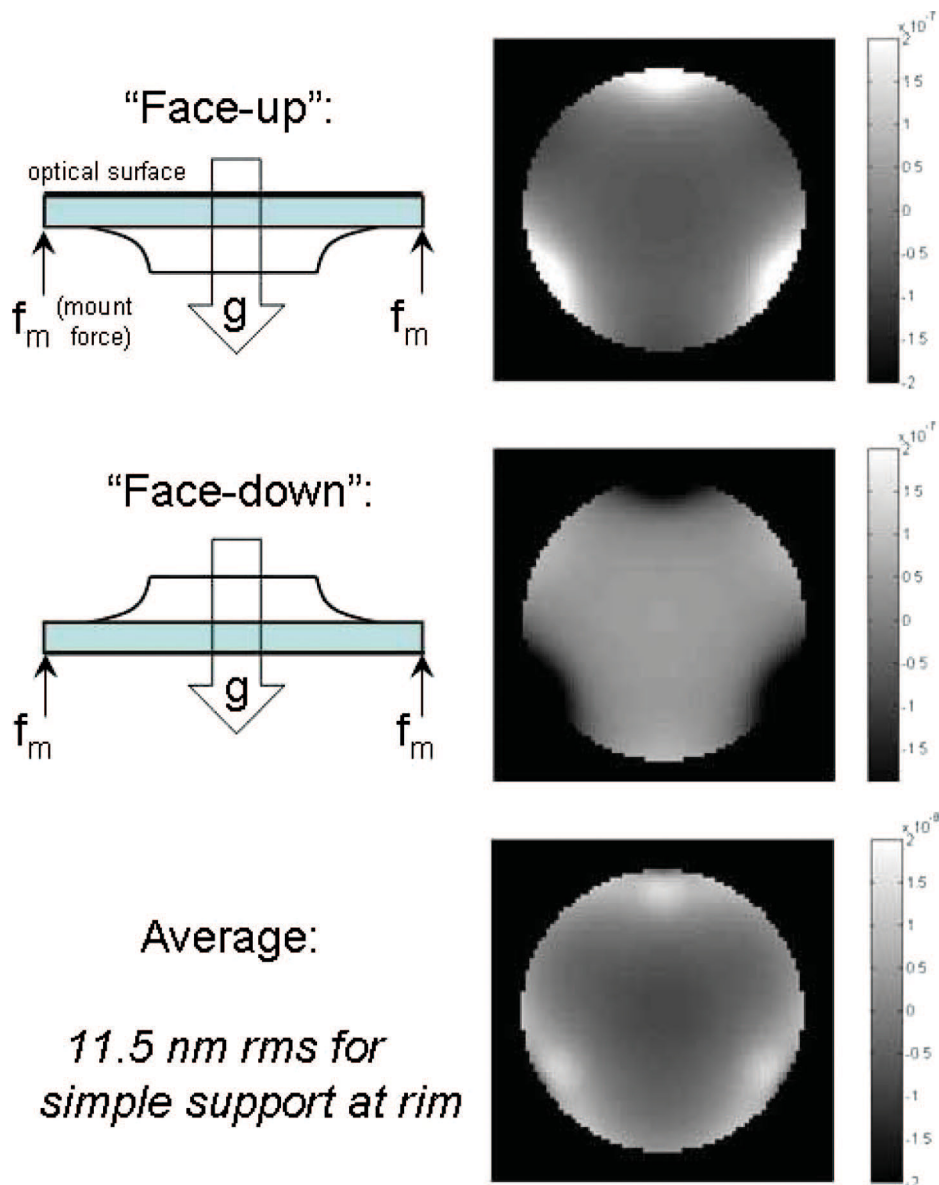


Fig. 3. (Color online) FEA modeling of the surface figure of PT-M1 during gravity reversal in a simple mirror mount in which the mirror rests on three points of contact near the rim (the threefold azimuthal symmetry is not depicted in the cartoons at left). The mirror model is specified to have a spherical surface in the absence of applied forces. The face-up and face-down orientations experience gravity forces that are reversed. However, mount forces in the two cases are applied at positions separated by the thickness of the mirror rim, so are only imperfectly reversed. Deformations in the two configurations are shown in the top two panels; their average is shown in the bottom panel, which recovers the ideal spherical surface (which would look flat in this display of departure from sphericity) marred by some simple artifacts near the rim. The rms error in the average is 11.5 nm.

removing the effects of gravity sag that will result will eliminate the need for modeling. In this section we motivate the basic technique of extracting the zero-gravity surface from two gravity-reversed orientations and extend the arguments to show that mount forces must also reverse for accurate results.

A. Reversal of Body Forces and Mount Forces

The fundamental solid-body equations can be cast in a form familiar from the FEA approach [6,7]. The three-dimensional solid body (mirror) is approximated by a mesh of N points, and positions of these points (nodes) are represented by a $3N$ -dimensional

coordinate vector \mathbf{x}_i . In the absence of forces, node positions are described by the zero-gravity position vector \mathbf{x}_i^{0g} that we wish to extract. Forces, also represented by a $3N$ -dimensional vector \mathbf{f}_i , cause deformations $\delta\mathbf{x}_i$ from the zero-gravity mirror shape; the case of interest is normal gravity ($1g$), for which we may write the altered positions as

$$\mathbf{x}_i^{1g} = \mathbf{x}_i^{0g} + \delta\mathbf{x}_i. \quad (1)$$

For our purposes, these forces may be either body forces due to gravity (\mathbf{f}^g) or boundary forces due to the mirror mount (\mathbf{f}^m). By a fundamental equation famil-

iar in FEA, the displacements are then found from

$$\mathbf{A}_{ij} \cdot \delta \mathbf{x}_j = \mathbf{f}_i = \mathbf{f}_i^g + \mathbf{f}_i^m, \quad (2)$$

where paired indices are summed over in the usual convention and \mathbf{A}_{ij} is the “stiffness matrix.” The stiffness matrix is generally sparse, so that a given node is significantly affected only by a small number of other, nearby nodes; with suitable numbering, it will be nearly diagonal. The stiffness matrix is a property of the geometry and material of the mirror itself and

so does not change when the mirror is rotated among orientations. Rotating the mirror into a new orientation in which body forces due to gravity reverse direction, and assuming that mount forces reverse as well, the new set of displacements $\delta \mathbf{x}'_j$ now obey

$$\mathbf{A}_{ij} \cdot \delta \mathbf{x}'_j = \mathbf{f}'_i = -\mathbf{f}_i^g - \mathbf{f}_i^m, \quad (3)$$

in the frame of the mirror. Comparing to Eq. (2) shows that

$$\delta \mathbf{x}'_j = -\delta \mathbf{x}_j \quad \text{for all } j. \quad (4)$$

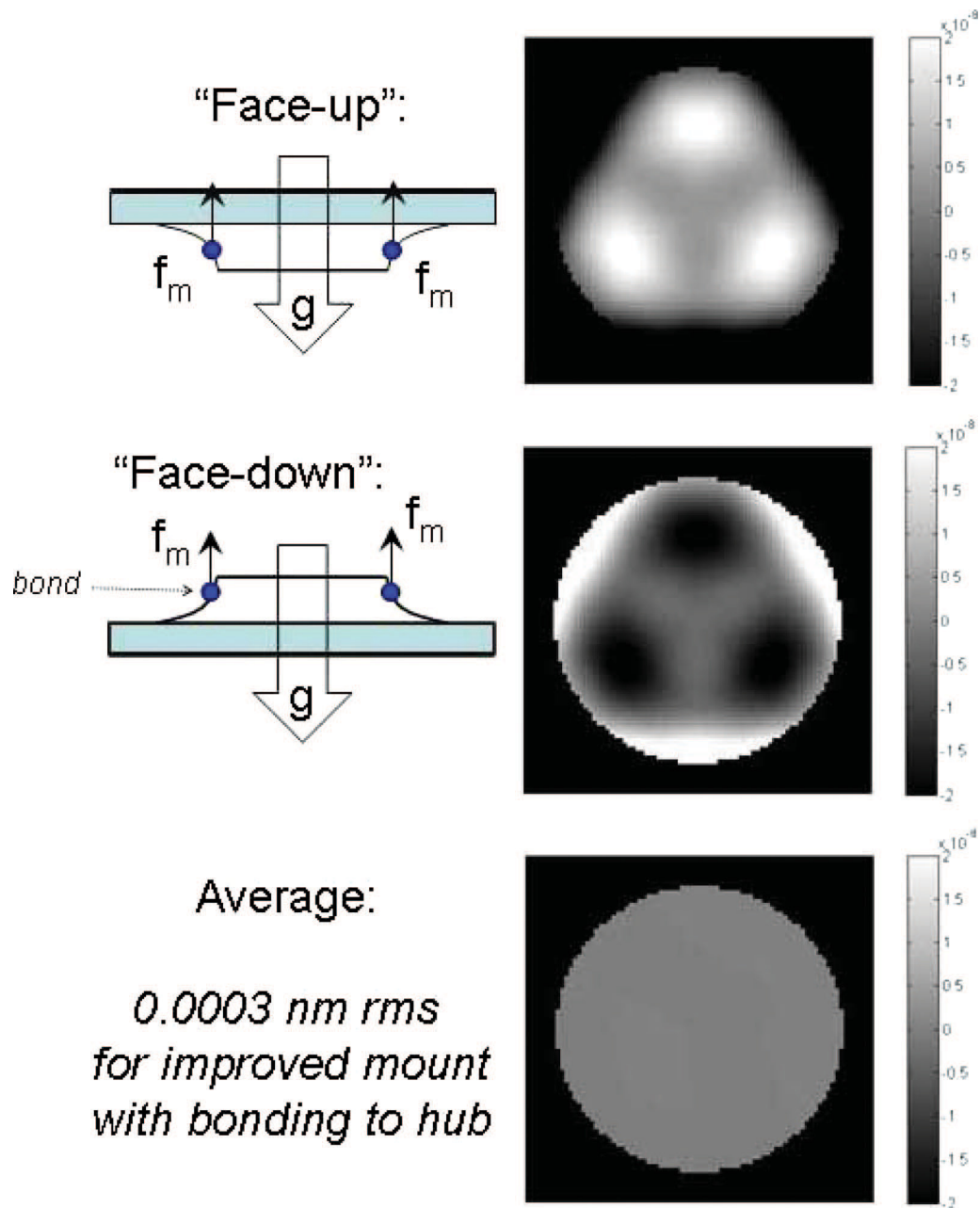


Fig. 4. (Color online) FEA modeling of the surface figure of PT-M1 during gravity reversal in an improved scheme incorporating the principles of Section 4. The mount now consists of three point contacts bonded to the hub at the back of the mirror (cartoons at left, but with threefold azimuthal symmetry, not depicted); mount forces thus reverse and are applied at very nearly the same positions in the two orientations, far from the mirror surface. As a result, the surface figures (top two panels at right) are nearly exactly complementary, giving an average map (lower right panel) with a formal rms error of only 0.0003 nm.

In other words, the average of the deformations from the ideal zero-gravity mirror shape in the two orientations is zero, so the average figure is just the zero-gravity surface. Algebraically, this property may be expressed as

$$\frac{1}{2}(\mathbf{x}_i^{1g} + \mathbf{x}_i^{1g'}) = \frac{1}{2}(\mathbf{x}_i^{0g} + \delta\mathbf{x}_i + \mathbf{x}_i^{0g} + \delta\mathbf{x}_i') = \mathbf{x}_i^{0g}. \quad (5)$$

If forces do not reverse perfectly, localized surface irregularities or dimples will be found on the mirror, as in Section 3. Precise reversal of gravity is relatively easy to achieve, but some care must be taken to ensure that mount forces f_i^m also reverse. Mount forces must not only reverse direction between the two gravity-reversed configurations, but the mount forces must be applied at the same points i of the mirror within the limits discussed in Subsection 4.B.

B. Mounting Attachment Points: the St. Venant Principle

In Subsection 4.A it was shown that mount forces, along with the body force due to gravity, should be reversed between the two orientations whose average will give the zero-gravity surface of the mirror. It is clear from the form of Eq. (2) that the reversed mount forces must act on the same nodes, i.e., at the same positions on the mirror. In this section we will show that mount forces need act at the same position to within only rather generous tolerances defined by the St. Venant principle.

The St. Venant principle captures a basic annealing or space-averaging property of elliptic partial differential equations, such as those governing solid-body deformations within the usual elastic, small-deformation regime. As quoted in [8], the principle states: “If a system of forces acting over ‘small’ areas of a solid are replaced by a statistically equivalent system (same force and moment) then the stresses change ‘significantly’ only in the ‘neighborhood’ of the loaded region.” Though rather qualitative as given, with no rigorous definitions for the quantities in single quotation marks, the St. Venant principle is nonetheless a powerful guide in choosing mutually inverted mount configuration pairs whose average gives the zero-gravity mirror surface. In this context, an error in mount position in the inverted orientation is unimportant if it is small compared to the distance to the optical surface of the mirror. Roughly speaking, small position errors are insignificant at distances through the glass of only 1.5 times their value [8], owing to the damping properties of the elliptic partial differential equations describing deformations in the glass. In retrospect, this principle accounts for the relatively good results that the simple mount scheme in Section 3 (Fig. 3) obtains in the central part of the mirror: that region is distant from the mount contact points by many times the distance scale separating the contact points in the two orientations.

C. Improved Mounting Scheme for PT-M1

The principles of Subsections 4.A and 4.B were applied to devise an improved gravity-reversed pair of

mirror mountings that more closely reverse mount forces as well. For determining PT-M1’s zero-gravity surface, the St. Venant principle implies that mounting points should be chosen far from the mirror surface of interest, i.e., on the lightweighted “hub” on the back of the mirror. To reverse mount forces as accurately as possible, one might place mount supports at three equispaced points on the side of the hub, as shown in Fig. 4, and attach them by bonding. This improved scheme results in a substantially more accurate measurement of the zero-gravity mirror surface, as the validation with FEA modeling in Fig. 4 shows. The face-up and face-down error maps are essentially inverses of each other, so their average is a flat error map whose rms deviation over the whole surface is nominally less than a picometer, far below the 6.3 nm rms level desired for PT-M1 testing.

The improved mounting scheme just described was implemented in hardware and surface metrology measurements were carried out with the PT-M1 prototype mirror (Fig. 5). Agreement with theoretical expectations was excellent: face-up and face-down surface deviations formed essentially complementary patterns, as desired, and measured 11.7 and 12.0 nm rms respectively, compared to values from

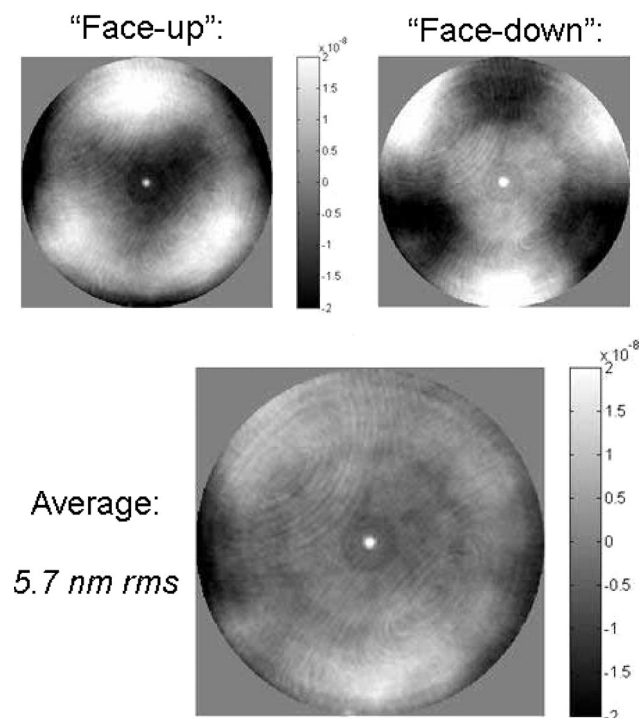


Fig. 5. Nanometer-scale optical surface metrology of the actual PT-M1 mirror for the face-up (upper left) and face-down (upper right) configurations; as with the modeling of Fig. 4, these are very nearly complementary to each other. The lower panel shows the average of the two, which gives the zero-gravity mirror figure; it departs from a spherical surface by only 5.7 nm rms. Included in this value are the surface errors of a fold flat in the optical train and some known imperfections in the mounts. The central spot is high by perhaps 35 nm but covers too small an area to have significant impact on the rms. [Metrology data courtesy S. Spanjian, T. Roff, L. Dettmann, and J. Daniel, Tinsley.]

FEA modeling of 14.9 nm rms for both orientations. Averaging the two maps yields a net zero-gravity surface deviation from the desired spherical figure of 5.7 nm rms. Presumably, then, this surface error largely reflects fabrication errors causing the mirror to depart from a perfect sphere in zero gravity. It also includes a small contribution from a 1.3 nm rms fold flat mirror used in the test optical train, any imperfections in the metrology interferometer's transmission sphere, and some effects apparently due to imperfectly fabricated mounts.

5. Simple, Near-Optimal On-Edge Mount for the PT-M1 Mirror

The considerations presented in Section 4 suggested a simple mounting scheme not requiring bonding

that might be used during the fabrication of the optic to provide a convenient zero-gravity error map as the surface is polished to its target shape. In this scheme, the mirror is oriented edge-on and is supported by two simple peg mounts contacting the ribs in the lightweighting structure in the back (the center of gravity of the PT-M1 mirror design is accessible to such pegs). Note that these pegs are much closer to the vertical center of the mirror than were the pegs used to support the TOM3 brassboard M1 discussed in Section 2, simplifying approximate reversal of mount forces in the present case. Note also that simple supports must be placed near the center of gravity of the mirror for accurate force reversal, but they may then for some mirror designs be relatively near the optical surface of the mirror, perhaps tending to con-

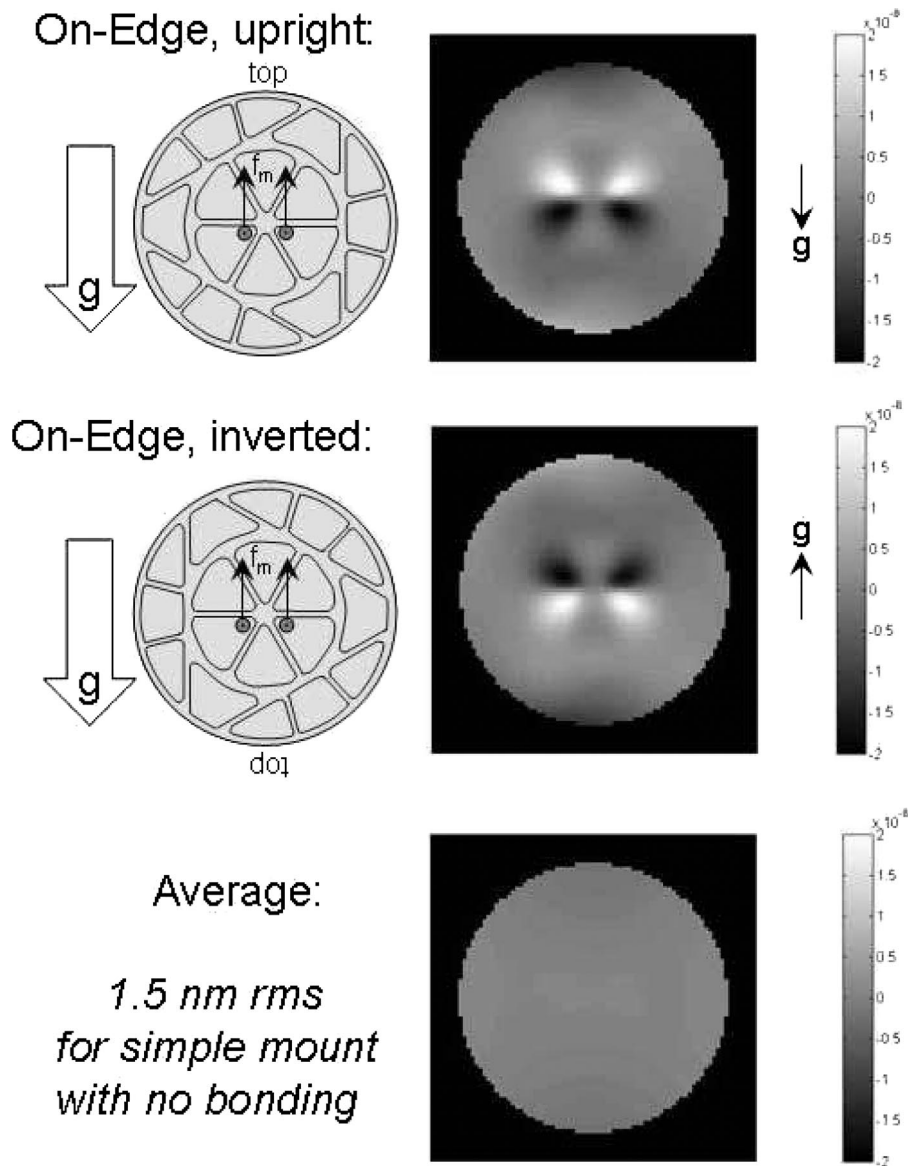


Fig. 6. FEA modeling of the surface figure of PT-M1 for a simple, near-optimal, on-edge gravity-reversal mounting scheme that can conveniently be implemented during the fabrication cycle. Two horizontal pegs under lightweighting ribs, near the vertical center, provide support. The average map (lower panel) has an rms error of only 1.5 nm. All figure panels at right are fixed in the frame of the optic; arrows indicate the direction of gravity.

flict with the St. Venant principle requirement that mount forces be applied some distance from that surface to reduce sensitivity to mounting errors.

As illustrated in Fig. 6, a 180° rotation of the mirror will cause the mount forces to reverse in direction and act at almost the same positions in each configuration, so one would expect the averaging technique to yield an accurate zero-gravity map. Indeed, while individual configurations in Fig. 6 have modeled surface deformations of ~ 4.9 nm rms, pair averages of these have deformations of only 1.5 nm rms. This is an acceptable level of error in the technique to enable studying a mirror surface with a target accuracy of $\lambda/100$ or 6.3 nm rms, as is the case with our PT-M1 optic. The mounting scheme proposed here is simple, requiring no bonding of mirror to mount, and no detailed knowledge of mount or mirror (only that the mount forces are the same in the two clocked orientations). This on-edge configuration is more convenient for optical testing than a face-up/face-down configuration, particularly when the mirror under test is an off-axis paraboloid: the focus is now easily accessible in a horizontal plane at the same height as

the mirror, to either side in the two orientations. This scheme might be particularly useful for inspection of the optic during the polishing stage, when optical surface testing is alternated with polishing, because it is easy to implement and requires no bonding. (It was in fact used during the fabrication cycle of the spherical PT-M1.)

The on-edge configurations just described were used in postfabrication acceptance testing of the spherical PT-M1 with excellent results (Fig. 7). In fact, six clockings (orientations) successively rotated by 60° were measured; these were conveniently accessible because of the sixfold symmetry of the mirror lightweighting. Three sets of 180° -rotated measurement pairs result. Individual surface maps have measured surface deformations of ~ 6 nm rms, and the “jet” structures seen in FEA modeling (Fig. 6) at the center of the mirror, near the mounting points, are reproduced in considerable detail. The average of all six measured configurations gives a surface map with a deformation of 3.8 nm rms, well within the target zero-gravity surface error of 6.3 nm rms.

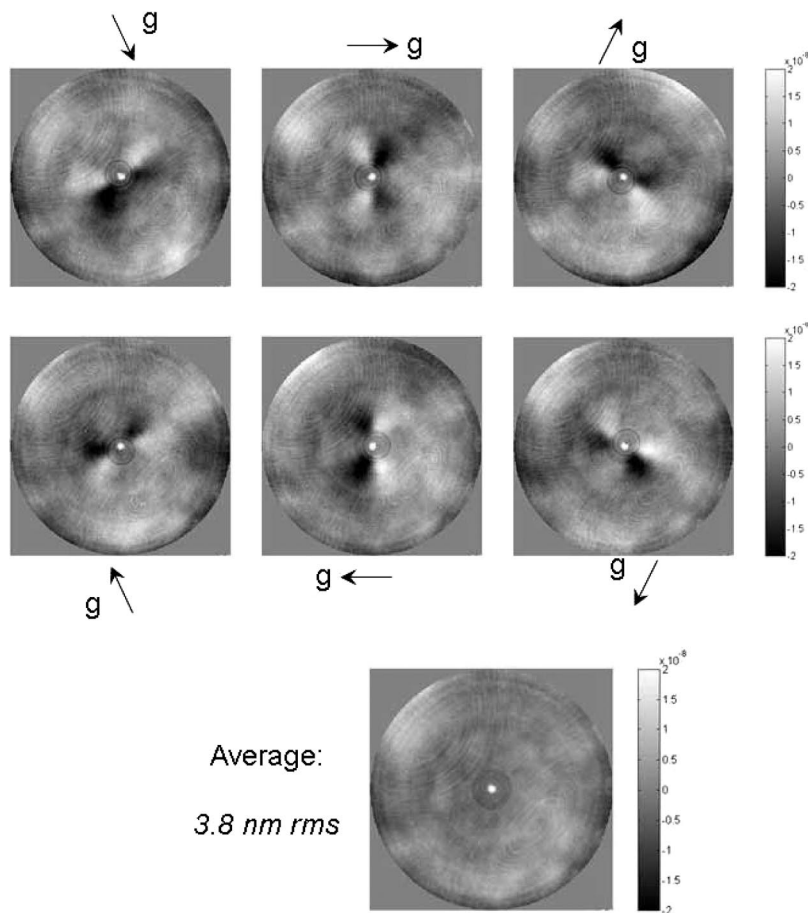


Fig. 7. Nanometer-scale optical surface metrology (upper panels) of the actual PT-M1 mirror for six different clockings of the near-optimal on-edge mount modeled in Fig. 6, showing a strong resemblance to the FEA modeling of Fig. 6. Each successive clocking is rotated by an angle of 60° . The lower map is the average of all six clockings, representing three gravity-reversed pairs; it departs from a sphere by only 3.8 nm rms. All figure panels are fixed in the frame of the optic; arrows indicate the direction of gravity. [Metrology data courtesy S. Spanjian, T. Roff, L. Dettmann, and J. Daniel, Tinsley.]

6. Conclusion

The classical technique for deducing the zero-gravity surface of a mirror is well known: average two surfaces measured in normal gravity at two orientations that cause gravity (body) forces to reverse. In the current paper we have elaborated on this technique to achieve accurate zero-gravity surface determinations, based on explicitly ensuring that the two normal-gravity orientations to be averaged have precisely reversed mount forces as well. In practice, mount forces must be applied at the same position in the two orientations to within an accuracy set by the St. Venant principle, which can be a relatively lenient restriction. We have illustrated and validated our technique by using finite-element analysis (FEA) to predict the response of SIM's prototype M1 (PT-M1) mirror at various orientations; however, the technique itself does not rely on FEA, and will generally yield results more accurate than FEA modeling of mount forces that are necessarily uncertain. The technique in fact obviates the need for accurate knowledge of the mount forces, requiring only that they be equal in magnitude and reversed in direction between the two orientations. Though the transition to a flightlike mount is somewhat beyond the scope of this paper, we note that preliminary test results on PT-M1 after coating and mounting in its flightlike mount indicate a surface figure consistent with the 6.3 nm rms design goal that was seen at earlier stages with the mirror deployed in test mounts. The techniques presented in this paper may be used to verify the zero-gravity surface figure of a mirror, whether in the fabrication cycle or during final ac-

ceptance testing, and proper mount design will then preserve that figure in its ultimate flightlike mount.

We thank Steve Macenka for helpful comments emphasizing the value of acceptance tests based on gravity-reversed measurements. Photographs of PT-M1 during fabrication (Fig. 1) and surface metrology data (Figs. 5 and 7) were provided by Stephanie Spanjian, Titus Roff, Lee Dettmann, and Jay Daniel of L-3 Communications Corp. SSG-Tinsley Division (Tinsley). The research described in this publication was carried out at the Jet Propulsion Laboratory, California Institute of Technology, under a contract with the National Aeronautics and Space Administration.

References

1. M. Shao, "Science overview and status of the SIM project," Proc. SPIE **5491**, 328–333 (2004).
2. R. A. Laskin, "Successful completion of SIM-PlanetQuest technology," Proc. SPIE **6268**, 626823 (2006).
3. D. Korsch, *Reflective Optics* (Academic, 1991).
4. R. Goullioud, "Results from the TOM3 testbed: thermal deformation of optics at the picometer level," presented at the *IEEE Aerospace Conference, Big Sky, Montana* (IEEE, 2006).
5. V. A. Feria, J. C. Lam, and D. Van Buren, "M1 mirror print-thru investigation and performance on the thermo-opto-mechanical testbed for the Space Interferometry Mission," Proc. SPIE **6273**, 62731C (2006).
6. Z. Chen, *Finite Element Methods and Their Applications* (Springer-Verlag, 2005).
7. D. W. Nicholson, *Finite Element Analysis: Thermomechanics of Solids* (CRC, 2003).
8. R. Richards, Jr., *Principles of Solid Mechanics* (CRC, 2001).